CHIN. PHYS. LETT. Vol. 29, No. 5 (2012) 052101

High-Spin States in Transuranium Nuclei ^{242,244}Pu *

ZHAO Yue(赵越)[1], KANG Xu-Zhong(康旭忠)[1], SHEN Shui-Fa(沈水法)[1,2,3,4,5**], YAN Yu-Peng(阎玉鹏)[2,6], HE Chuang-Ye(贺创业)[7], YAN Shi-Wei(晏世伟)[8]

[1]*Engineering Research Center of Nuclear Technology Application (Ministry of Education), East China Institute of Technology, Nanchang 330013*
[2]*School of Physics, Suranaree University of Technology, Nakhon Ratchasima 30000, Thailand*
[3]*International Centre for Materials Physics, Chinese Academy of Sciences, Shenyang 110016*
[4]*Fundamental Science on Radioactive Geology and Exploration Technology Laboratory, East China Institute of Technology, Fuzhou 344000*
[5]*State Key Laboratory of Nuclear Physics and Technology, Peking University, Beijing 100871*
[6]*Thailand Center of Excellence in Physics (ThEP), Commission on Higher Education, 328 Si Ayutthaya Road, Ratchathewi, Bangkok 10400, Thailand*
[7]*China Institute of Atomic Energy, P.O. Box 275(10), Beijing 102413*
[8]*College of Nuclear Science and Technology, Beijing Normal University, Beijing 100875*

(Received 31 October 2011)

We investigate the structure of yrast bands in the transuranium nuclei ^{242}Pu and ^{244}Pu in the framework of the projected shell model, which is a fully quantum mechanical and microscopic approach. It is found that an appropriate modification of the standard Nilsson spin-orbital parameters in the $N = 6$ proton shell is necessary to correctly describe the high-spin backbending phenomenon in nucleus ^{244}Pu. In order to test whether this modification is correct, the same modified parameters are used to calculate the yrast band of its neighboring isotope ^{242}Pu. It is found that without this modification, a backbending will occur at spin $I = 20$, which is not supported by the experimental data.

PACS: 21.60.Cs, 21.10.Re, 27.90.+b DOI: 10.1088/0256-307X/29/5/052101

The investigation of nuclear high-spin states began in the 1970s when the backbending phenomenon was discovered in some well-deformed nuclei.[1,2] In the transuranium region, the backbending phenomenon in an actinide nucleus ^{244}Pu was first observed by Spreng *et al.*[3] in 1983. In recent years, the higher spin states in transuranium nuclei have been measured with greater accuracy as advanced accelerators and high-resolution detectors are now available. Theoretical predictions of existing transuranium nuclei are based on the calculated properties of heavy nuclei as a function of the location of single-particle orbitals within deformed potentials.[4] Transuranic nuclei furnish a testing ground for these theories where the calculated properties may be compared with experimental data.

The conventional shell model is not an optimal way to describe the properties of transuranium nuclei because of their huge configuration. On the other hand, we have never been interested in a complete description of the system, that is, it is very important to limit our interest to a certain class of states. The projected shell model (PSM) is carried out using a set of few, well-selected configurations, and it has been used to describe the high-spin states of yrast bands of even–even rare-earth nuclei quite successfully.[5–7] In this work, we want to employ this model to study the high-spin phenomenon of transuranium nuclei. In recent years, experimental data in the transfermium region, which has the mass number A, greater than that of the transuranium region, are constantly emerging, and some corresponding theoretical works have been published (see, e.g., Refs. [8,9]). The investigation of this region has an important significance for studying the synthesis and structure of superheavy nuclei (SHN). The confirmation of the Nilsson single-particle level sequence and deformation parameters is very important to describe the nuclear property in this region. To date, the rotational ground state bands in some nuclei in this region have been observed but rarely up to the backbending (band crossing) region.

In view of an extensive review article giving a detailed description of the PSM (see Ref. [10]), we only briefly describe the main framework of this model here. The PSM is a spherical shell model built on a deformed basis. The PSM calculation usually begins with the deformed Nilsson single-particle states at a deformation of ε_2. Pairing correlations are incorporated into the Nilsson single-particle states by BCS calculations. The results of the Nilsson-BCS cal-

*Supported by Suranaree University of Technology under Grant No 15/2553, the National Basic Research Development Program of China under Grant No 2007CB815003, the National Natural Science Foundation of China under Grant Nos 10975190, 11065001, 10975019, 10675170 and 61067001.
**Correspondence author. Email: shfshen@ecit.cn
© 2012 Chinese Physical Society and IOP Publishing Ltd

culations provide us with a set of quasi-particle (qp) states that define the qp vacuum $|\Phi(\varepsilon_2)\rangle$. One then constructs the shell-model basis by building multi-qp states. The broken symmetry in these states is recovered by angular momentum projection (and particle number projection, if necessary) to form a shell-model basis in the laboratory frame. Finally, a two-body shell-model Hamiltonian is diagonalized in the projected space.

Following the spirit of the Tamm–Dancoff method,[11] we build the shell-model space by including 0-, 2-, and 4-qp states for an even–even nucleus:

$$|\Phi_k\rangle = \{|0\rangle, a^+_{n_i}a^+_{n_j}|0\rangle, a^+_{p_i}a^+_{p_j}|0\rangle, a^+_{n_i}a^+_{n_j}a^+_{p_i}a^+_{p_j}|0\rangle\}, \tag{1}$$

where a^+ is the creation operator for a qp, and subscripts $n\,(p)$ denote neutron (proton) Nilsson quantum numbers which run over the low-lying orbitals. The bases in Eq. (1) are not arbitrarily selected but are taken from all the neutron and proton Nilsson orbitals that lie close to the Fermi surface. Thus, the projected multi-qp states are the building blocks of the shell model basis:

$$|\psi^I_M\rangle = \sum_k \mathrm{f}^{\mathrm{I}}_{\mathrm{k}} \hat{P}^I_{MK}|\Phi_k\rangle, \tag{2}$$

where k labels the basis states and $\mathrm{f}^{\mathrm{I}}_{\mathrm{k}}$ values are determined by configuration mixing. We then diagonalize the Hamiltonian in the projected multi-qp states given in Eq. (2). In the calculation, we employ a quadrupole plus a pairing Hamiltonian, with the inclusion of a quadrupole-pairing term:

$$\hat{H} = \hat{H}_0 - \frac{1}{2}\chi\sum_\mu \hat{Q}^+_\mu\hat{Q}_\mu - G_M\hat{P}^+\hat{P} - G_Q\sum_\mu \hat{P}^+_\mu\hat{P}_\mu, \tag{3}$$

where $\hat{H}_0$ is the spherical single-particle Hamiltonian which contains a proper spin-orbital force:

$$\hat{H}_0 = \sum_\alpha c^+_\alpha \varepsilon_\alpha c_\alpha,$$
$$\varepsilon_\alpha \equiv \hbar\omega\{N - \kappa[2\boldsymbol{j}\cdot\boldsymbol{s} + \mu(\boldsymbol{l}^2 - \langle\boldsymbol{l}^2\rangle)]_{Nj}\}. \tag{4}$$

The other terms in Eq. (3) are quadrupole–quadrupole, and monopole- and quadrupole-pairing interactions, respectively. The quadrupole–quadrupole interaction strength χ is adjusted such that the known input quadrupole deformation ε_2 is obtained as a result of self-consistent mean-field calculations.[10] The monopole pairing strength constant G_M is taken to be $G_M = [20.45 \mp 13.86(N - Z)/A]/A$, with $-$ for neutrons and $+$ for protons, which more or less reproduces the observed odd–even mass differences in this mass region. This choice of G_M is appropriate for the single-particle space employed in the PSM, where three major shells are used for each type of nucleon, i.e., N=5, 6, 7 for neutrons and $N = 4$, 5, 6 for protons. The quadrupole pairing strength G_Q in Eq. (3) is assumed to be 13% of the monopole pairing G_M, which is found to be appropriate for transuranium nuclei.[12,13]

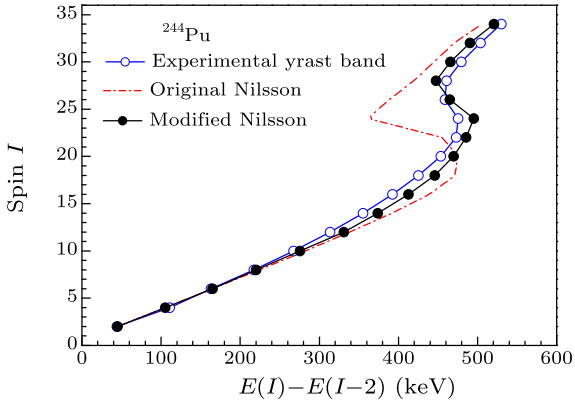

Fig. 1. Spin vs yrast band transition energy plot for ^{244}Pu. Two theoretical calculations which differ in the Nilsson parameters for the $N = 6$ proton shell are compared with the experimental data.[21]

The spin-orbital force parameters κ and μ, appearing in the Nilsson model, are essential in reproducing a correct shell filling. They are also important for the excited configurations in the even–even nuclei, as we shall see in the current work. In the calculations for actinides, one usually uses the compilation made by Nilsson *et al.*[14] (A-dependent) although it is not deduced from the actinide region. This is why in the present calculations we also allow the parameters κ and μ, slightly different from the Nilsson version. There are also other compilations of the parameters κ and μ. Bengtsson and Ragnarsson[15] refitted these parameters to the experimental data available then and derived different values for different main oscillator quantum numbers, rather than A. The parameters κ and μ in Ref. [15] were later revised by Zhang *et al.* for the proton $N = 5$, 6 major shells in the Au-Pt region[16] and for the proton $N = 4$, 5, 6 major shells in the $A \approx$120–140 region,[17] respectively. Sun *et al.*[18] also proposed a new set of Nilsson parameters for proton-rich nuclei with proton and neutron numbers $28 \leq N(Z) \leq 40$. Seo[19] introduced N- and l-dependent κ and μ for a broad range of the mass region. The quadrupole deformation parameters ε_2 and hexadecapole deformation parameters ε_4 are taken from the compilation of Möller *et al.*[20]

In Fig. 1, we show the backbending plot of the yrast band of ^{244}Pu. The experimental data was compared with two theoretical calculations which differ in the proton Nilsson parameters in the $N = 6$ shell. In both the theoretical calculations, the experimental data are nicely reproduced until $I = 12$. However, one of these results (dot-dashed line in Fig. 1), obtained by the Nilsson parameters adopted from Ref. [14] for proton $N = 4$, 5, 6 major shells $\kappa = 0.0576$ and $\mu = 0.651$,

exhibits a strong backbending phenomenon at $I = 20$. Obviously, this predication is not supported by the experimental data. On the other hand, the second theoretical result (filled circles in Fig. 1 obtained by modifying the Nilsson parameters) nicely describes the experimental backbending phenomenon at spin $I = 26$, and reproduces the experimental data for the entire region of spin I.

One of the motivations of the current work is to find out why the calculated backbending occurs at different positions for different Nilsson parameters κ and μ. For this purpose, the band diagram[10] is the most appropriate tool as it shows the detailed behavior of various bands as a function of spin I.

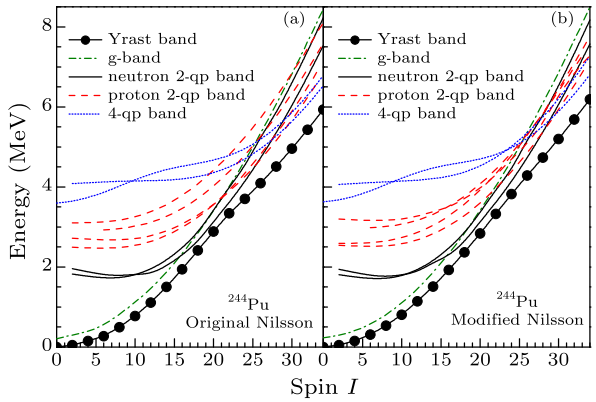

Fig. 2. Band diagram for the positive parity states in ^{244}Pu: (a) using the original Nilsson parameters, (b) using the modified ones for the proton $N = 6$ shell. Their configurations (from bottom to top in accordance with the bandheads) are listed in the text.

The band diagrams corresponding to the two above-mentioned theoretical results are shown in Fig. 2. It can be seen from Figs. 2(a) and 2(b) that at first the yrast band smoothly follows the g-band until spin $I = 16$. This behavior is interrupted at this spin by a band crossing with a neutron 2-qp band. The crossing angle is small and thus nothing drastic can occur around the crossing spin. These bands are built upon neutron 2-qp states from the $j_{15/2}$ shell and are important for yrast band evolution. Their configurations are (from lowest to highest in accordance with the bandheads) $j_{15/2}[\frac{9}{2}^-, -\frac{11}{2}^-]K^\pi = -1^+$ and $j_{15/2}[-\frac{7}{2}^-, \frac{9}{2}^-]K^\pi = 1^+$. There are also 2-qp (two quasiproton) and 4-qp (two quasiproton + two quasineutron) bands with the configurations: (a) $\pi i_{13/2}[\frac{5}{2}^+, -\frac{7}{2}^+]K^\pi = -1^+, \pi i_{13/2}[-\frac{3}{2}^+, \frac{5}{2}^+]K^\pi = 1^+, \pi i_{13/2}[-\frac{3}{2}^+, -\frac{7}{2}^+]K^\pi = -5^+, \pi i_{13/2}[-\frac{7}{2}^+, \frac{9}{2}^+]K^\pi = 1^+, \nu j_{15/2}[-\frac{7}{2}^-, \frac{9}{2}^-] \oplus \pi i_{13/2}[\frac{5}{2}^+, -\frac{7}{2}^+]K^\pi = 0^+, \nu j_{15/2}[-\frac{7}{2}^-, \frac{9}{2}^-] \oplus \pi i_{13/2}[-\frac{3}{2}^+, \frac{5}{2}^+]K^\pi = 2^+$; (b) $\pi i_{13/2}[\frac{5}{2}^+, -\frac{7}{2}^+]K^\pi = -1^+, \pi i_{13/2}[-\frac{7}{2}^+, \frac{9}{2}^+]K^\pi = 1^+, \pi i_{13/2}[-\frac{3}{2}^+, -\frac{7}{2}^+]K^\pi = -5^+, \pi i_{13/2}[-\frac{3}{2}^+, \frac{5}{2}^+]K^\pi = 1^+, \nu j_{15/2}[-\frac{7}{2}^-, \frac{9}{2}^-] \oplus \pi i_{13/2}[\frac{5}{2}^+, -\frac{7}{2}^+]K^\pi = 0^+, \nu j_{15/2}[-\frac{7}{2}^-, \frac{9}{2}^-] \oplus \pi i_{13/2}[-\frac{7}{2}^+, \frac{9}{2}^+]K^\pi = 2^+$.

In Fig. 2(a), the sharp band crossing is seen at approximately spin $I = 20$, where two proton bands $\pi i_{13/2}[\frac{5}{2}^+, -\frac{7}{2}^+]K^\pi = -1^+$ and $\pi i_{13/2}[-\frac{3}{2}^+, \frac{5}{2}^+]K^\pi = 1^+$ cross the g-band simultaneously. This sharp crossing is the source of our wrongly predicted backbending of the yrast band. Another two proton bands $\pi i_{13/2}[-\frac{3}{2}^+, -\frac{7}{2}^+]K^\pi = -5^+$ and $\pi i_{13/2}[-\frac{7}{2}^+, \frac{9}{2}^+]K^\pi = 1^+$ cross the g-band in a very gentle way at spins $I = 26$ and $I = 30$, respectively. The 4-qp band $\nu j_{15/2}[-\frac{7}{2}^-, \frac{9}{2}^-] \oplus \pi i_{13/2}[-\frac{3}{2}^+, \frac{5}{2}^+]K^\pi = 2^+$ becomes most important for the yrast band above the spin $I = 30$.

It is clear that wrong prediction of the backbending can be avoided if the positions of the proton 2-qp bands are shifted properly. The relative positions of various excited bands in a nucleus are sensitive to the deformed single-particle energies as determined by the Nilsson potential. Based on this consideration, we have modified the Nilsson parameters κ and μ for the $N = 6$ proton shell (which contains the $i_{13/2}$ subshell) by simply multiplying a factor of 1.12, namely we have increased these parameters by 12%. The resulting backbending plot is denoted as "modified Nilsson" in Figs. 1 and 2(b).

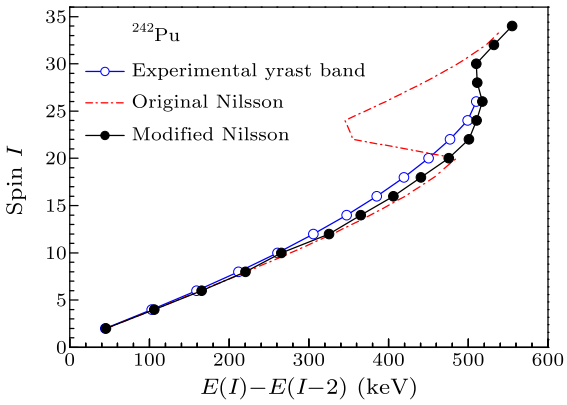

Fig. 3. Spin vs transition energy for ^{242}Pu. Two theoretical calculations which differ in the Nilsson parameters for the $N = 6$ proton shell are compared with the experimental data.[22]

In Fig. 2(b), we can see that this modification has little influence on the positions of g-band and neutron 2-qp bands. However, the situation is different for the proton 2-qp bands and 4-qp bands. In this case only one proton 2-qp band with configuration $\pi i_{13/2}[\frac{5}{2}^+, -\frac{7}{2}^+]K^\pi = -1^+$ crosses the g-band at about the spin $I = 22$, which causes only gentle backbending. Three proton bands with configurations $\pi i_{13/2}[-\frac{7}{2}^+, \frac{9}{2}^+]K^\pi = 1^+$, $\pi i_{13/2}[-\frac{3}{2}^+, -\frac{7}{2}^+]K^\pi = -5^+$, and $\pi i_{13/2}[-\frac{3}{2}^+, \frac{5}{2}^+]K^\pi = 1^+$ respectively then cross the g-band at about $I = 26$. These crossings are the source of the backbending of the yrast band of ^{244}Pu, which is observed in the experiment.[3] In

fact, the agreement with data in Fig. 1 (filled circles vs open circles) is achieved after this modification of the Nilsson parameters. Finally, the 4-qp band with configuration $\nu j_{15/2}[-\frac{7}{2}^-, \frac{9}{2}^-]\oplus\pi i_{13/2}[\frac{5}{2}^+, -\frac{7}{2}^+]K^\pi = 0^+$ becomes most important for the yrast band above the spin $I = 30$.

This might pose a question about the correctness of the (proton) Nilsson diagram which serves as a standard basis for the structure calculations. The original parameters used to generate the Nilsson diagram in this work were fitted more than 40 years ago[14] when there were not many high-spin data available. The Nilsson parameters for higher proton shells seem to be rather problematic and we feel it is necessary to study it. Whether this modification could describe the high-spin phenomenon of its neighboring isotope ^{242}Pu can prove its reasonability.

In Fig. 3, the experimental data are compared with two theoretical calculations which differ in the proton Nilsson parameters in the $N = 6$ shell. In both of the theoretical calculations, the experimental data are nicely reproduced until $I = 10$. The curve (dot-dashed line in Fig. 3) calculated using the original Nilsson parameters, i.e., for proton $N = 4$, 5, 6 major shells κ= 0.0577 and $\mu = 0.650$, exhibits a very strong backbending phenomenon at spin $I = 20$. On the other hand, the second theoretical result obtained by the same modification of the Nilsson parameters (filled circles in Fig. 3) reproduces the experimental data well. In addition, we predict that a very slight backbending exists between $I = 26$ and $I = 30$. Here we emphasize the necessity of the same modification in the proton Nilsson parameter for the $N = 6$ shell. Without this modification, a backbending would occur at spin $I = 20$, which is not supported by the data.

In summary, we have studied the structure of yrast bands in the transuranium nuclei ^{242}Pu and ^{244}Pu in the framework of the projected shell model, which is based on a fully quantum mechanical and microscopic theory. In this work, it has been found that an appropriate modification of the standard Nilsson spin-orbital parameters in the N=6 proton shell is necessary in order to correctly describe the backbending phenomenon in nucleus ^{244}Pu. Three proton bands with configurations $\pi i_{13/2}[-\frac{7}{2}^+, \frac{9}{2}^+]K^\pi = 1^+$, $\pi i_{13/2}[-\frac{3}{2}^+, -\frac{7}{2}^+]K^\pi = -5^+$ and $\pi i_{13/2}[-\frac{3}{2}^+, \frac{5}{2}^+]K^\pi = 1^+$ respectively, crossing the g-band at about $I = 26$ were found to be the source of the backbending of the yrast band of ^{244}Pu. In order to test this modification correctly, we used the same modified parameters to calculate the yrast band of ^{242}Pu. It was found that without this modification, a backbending would occur at spin $I = 20$, whereas the backbending is reproduced well when the modified parameters are used. In addition, we predict a very slight backbending between $I = 26$ and $I = 30$ in ^{242}Pu.

Finally, we would like to emphasize that the Nilsson spin-orbital parameters are very important for a correct theoretical description of the high-spin structure. In light of the quality and richness of high-spin data today, the current work suggests the necessity of a systematic reinvestigation of the Nilsson single-particle levels, which is the starting point of many theoretical models.

References

[1] Johnson A, Ryde H and Sztarkier J 1971 *Phys. Lett.* B **34** 605
[2] Johnson A, Ryde H and Hjorth S A 1972 *Nucl. Phys.* A **179** 753
[3] Spreng W, Azgui F, Emling H, Grosse E, Kulessa R, Michel Ch, Schwalm D, Simon R S, Wollersheim H J, Mutterer M, Theobald J P, Moore M S, Trautmann N, Egido J L and Ring P 1983 *Phys. Rev. Lett.* **51** 1522
[4] Nilsson B 1969 *Nucl. Phys.* A **129** 445
[5] Hara K and Sun Y 1991 *Nucl. Phys.* A **529** 445
[6] Zou W H and Gu J Z 2010 *Chin. Phys. Lett.* **27** 012101
[7] Sun Y and Hara K 1998 *Phys. Rev.* C **57** 3079
[8] He X T, Ren Z Z, Liu S X and Zhao E G 2009 *Nucl. Phys.* A **817** 45
[9] Zhang Z H, He X T, Zeng J Y, Zhao E G and Zhou S G 2012 arXiv:1110.6134v2[nucl-th]
[10] Hara K and Sun Y 1995 *Int. J. Mod. Phys.* E **4** 637
[11] Ring P and Schuck P 1980 *The Nuclear Many-Body Problem* (Berlin: Springer-Verlag) chap 8 p 282
[12] Sun Y, Long G L, Falih A K and Sheikh J A 2008 *Phys. Rev.* C **77** 044307
[13] Chen Y S, Sun Y and Gao Z C 2008 *Phys. Rev.* C **77** 061305
[14] Nilsson S G, Tsang C F, Sobiczewski A, Szymanski Z, Wycech S, Gustafson C, Lamm I L, Möler P and Nilsson B 1969 *Nucl. Phys.* A **131** 1
[15] Bengtsson T and Ragnarsson I 1985 *Nucl. Phys.* A **436** 14
[16] Zhang J Y, Larabee A J and Riedinger L L 1987 *J. Phys.* G **13** L75
[17] Zhang J Y, Xu N, Fossan D B, Liang Y, Ma R and Paul E S 1989 *Phys. Rev.* C **39** 714
[18] Sun Y, Zhang J Y, Guidry M, Meng J and Im S 2000 *Phys. Rev.* C **62** 021601
[19] Seo T 1986 *Z. Phys.* A **324** 43
[20] Möller P, Nix J R, Myers W D and Swiatecki W J 1995 *At. Data. Nucl. Data. Tables* **59** 185
[21] Akovali Y A 2003 *Nucl. Data Sheets* **99** 197
[22] Akovali Y A 2002 *Nucl. Data Sheets* **96** 177